Mon. Not. R. Astron. Soc. **368,** 1489–1499 (2006) doi:10.1111/j.1365-2966.2006.10238.x

Torus formation in neutron star mergers and well-localized short gamma-ray bursts

R. Oechslin⋆ and H.-T. Janka

Max-Planck-Institut für Astrophysik, Karl-Schwarzschild-Str. 1, D-85741 Garching, Germany

Accepted 2006 February 23. Received 2006 February 23; in original form 2005 July 6

ABSTRACT

Merging neutron stars (NSs) are hot candidates for the still enigmatic sources of short gamma-ray bursts (GRBs). If the central engines of the huge energy release are accreting relic black holes (BHs) of such mergers, it is important to understand how the properties of the BH–torus systems, in particular disc masses and mass and rotation rate of the compact remnant, are linked to the characterizing parameters of the NS binaries. For this purpose, we present relativistic smoothed particle hydrodynamic simulations with conformally flat approximation of the Einstein field equations and a physical, non-zero temperature equation of state. Thick disc formation is highlighted as a dynamical process caused by angular momentum transfer through tidal torques during the merging process of asymmetric systems or in the rapidly spinning triaxial post-merger object. Our simulations support the possibility that the first well-localized short and hard GRBs 050509b, 050709, 050724, 050813 have originated from NS merger events and are powered by neutrino-antineutrino annihilation around a relic BH–torus system. Using model parameters based on this assumption, we show that the measured GRB energies and durations lead to estimates for the accreted masses and BH mass accretion rates which are compatible with theoretical expectations. In particular, the low-energy output and short duration of GRB 050509b set a very strict upper limit of less than 100 ms for the time interval after the merging until the merger remnant has collapsed to a BH, leaving an accretion torus with a small mass of only $\sim$0.01 $M_\odot$. This favours a (nearly) symmetric NS+NS binary with a typical mass as progenitor system.

Key words: equation of state – hydrodynamics – relativity – stars: neutron – gamma-rays: bursts.

1 INTRODUCTION

Merger events of neutron star (NS)+NS or NS+black hole (BH) binaries do not only belong to the strongest known sources of gravitational wave (GW) radiation, but they are also widely favoured as the origin of the class of short, hard gamma-ray bursts (GRBs) (Blinnikov et al. 1984; Paczyński 1986; Eichler et al. 1989; Paczyński 1991; Narayan, Paczyński & Piran 1992). The recent first good localizations of short bursts, GRB 050509b, 050709, 050724, 050813, by the *Swift* and *Hete* satellites at redshifts between 0.160 and 0.722 (see Fox et al. 2005; Gehrels et al. 2005; Villasenor et al. 2005, and references therein) were interpreted as a possible confirmation of this hypothesis (Bloom et al. 2005; Fox et al. 2005; Hjorth et al. 2005a,b; Lee, Ramirez-Ruiz & Granot 2005), because the bursts have observational characteristics which are different from those of long GRBs, but which are in agreement with expectations for compact object mergers.

The central engines of such bursts are still poorly understood and observationally undetermined. But it seems unlikely that the energies required for typical short GRBs are set free during the dynamical phase of the merging of two NSs (Ruffert, Janka & Schäfer 1996). The production of GRBs by the neutrino emitting, hot post-merger NS is also disfavoured, because the high mass-loss rates in a neutrino-driven wind, which is caused by neutrino energy deposition near the NS surface, rules out the production of high Lorentz factor outflow (Woosley & Baron 1992; Woosley 1993a). Instead, the long-time accretion of a BH formed from a transiently stable, supramassive or hypermassive merger remnant [for definitions of these terms, see Morrison, Baumgarte & Shapiro (2004)] is a much more promising source (e.g. Woosley 1993b; Popham, Woosley & Fryer 1999; Ruffert & Janka 1999; Rosswog, Ramirez-Ruiz & Davies 2003; Lee, Ramirez-Ruiz & Page 2005), provided the BH is surrounded by a sufficiently massive accretion torus. Due to the geometry of the BH–torus system with relatively baryon-poor regions

⋆E-mail: roe@MPA-Garching.MPG.DE

along the rotation axis, thermal energy release preferentially above the poles of the BH by the annihilation of neutrino-antineutrino ($\nu\bar{\nu}$) pairs (Jaroszyński 1993; Mochkovitch et al. 1993) can lead to collimated, highly relativistic jets of baryonic matter with properties in agreement with those needed to explain short GRBs (Aloy, Janka & Müller 2005). Ultrarelativistic jets were found to develop if the rate of thermal energy deposition per unit solid angle is sufficiently large. Alternatively or in addition, magneto-hydrodynamic (MHD) field amplification in the rapidly spinning disc could drive polar jets, or magnetic coupling between the rotating BH and the girding accretion torus could tap the rotational energy of the BH (Blandford & Znajek 1977) and could help powering MHD-driven outflow (e.g. Brown et al. 2000; Drenkhahn & Spruit 2002).

Torus mass as well as BH mass and rotation are thus crucial parameters that determine the energy release from the merger remnant on the secular time-scale of the viscous evolution of the BH–torus system. In this paper, we present the first set of results from new three-dimensional (3D), relativistic smoothed particle hydrodynamic simulations of NS mergers with a physical equation of state (EoS), which aim at establishing the link between the remnant properties and those of the binary systems. Previous such attempts [see Baumgarte & Shapiro (2003) for a review] were either performed in the Newtonian limit (e.g. Ruffert & Janka 2001 and references therein; Rosswog et al. 2003), or with polytropic or otherwise radically simplified treatments of the high- and low-density EoSs and their temperature-dependent behaviour (e.g. Shibata, Taniguchi & Uryū 2003, 2005), or they considered disc formation by viscous or magnetic effects during the secular evolution of hypermassive NSs (Duez et al. 2004, 2005). Here, we instead highlight torus formation in NS mergers as a dynamical process and argue that this is consistent with the recent observations of short GRBs.

2 NUMERICAL METHODS AND MODELS

We employ an improved version of our relativistic smoothed particle hydrodynamics (SPH) code (Oechslin, Rosswog & Thielemann 2002; Oechslin et al. 2004), which solves the relativistic hydrodynamic equations together with the Einstein field equation in the conformally flat approximation (Isenberg & Nester 1980; Wilson, Matthews & Marronetti 1996). The code now allows for the use of a tabulated, non-zero temperature EoS and solves the energy equation in a form without explicit time derivatives of the metric elements on the right-hand side (RHS) (cf. Oechslin et al. 2002, equation A8). The properties of the stellar plasma are described by the non-zero temperature EoS of Shen et al. (1998a,b), which is used with baryonic density, internal energy and electron fraction (proton-to-baryon ratio) Y_e as input, and pressure and temperature as output. Since the backreaction of the neutrino emission on the stellar fluid is small on the time-scales considered here, we ignore neutrinos in our models. As a consequence, the electron fraction, Y_e, needed by the EoS as an input remains constant on the Lagrangian SPH particles. Details on the numerical scheme will be presented in Oechslin, Janka, & Marek (in preparation).

We start our simulations shortly before the tidal instability sets in and follow the evolution with typically 400 000 SPH particles through merging and torus formation until either the collapse of the merger remnant sets in or a quasi-stationary state has formed.

Initial conditions for our simulations are generated by placing two NSs in hydrostatic equilibrium on a circular orbit of a given orbital distance and by relaxing the configuration with the use of a small damping force into a circular orbital motion with an irrotational spin state. The orbital velocity is adjusted during this process in order to obtain the binary in orbital equilibrium. The initial electron fraction Y_e is obtained by requiring neutrinoless β-equilibrium for cold NS matter, i.e. we determine Y_e from the condition that the (electron) neutrino chemical potential μ_{ν_e} is equal to zero for a given density (and initial temperature $T \sim 0$).

We consider a variety of models with different NS masses and mass ratios. Other unknown parameters, such as the NS spins and the EoS, are kept fixed except for two models where thermal effects in the EoS are neglected. This is realized by reducing the EoS to the 2D slice at $T = 0$ with density and Y_e as input and pressure and internal energy as output. This reduction has no influence as long as shocks are absent, i.e. as long as the fluid evolves adiabatically. In the presence of shocks, however, the $T = 0$ case corresponds to the extreme situation that a very efficient cooling mechanism immediately extracts the entropy and internal energy generated in shocks.

In Table 1, the key parameters characterizing our different models are summarized. We have investigated NS+NS binaries with mass ratios q between 0.55 and unity, roughly covering the theoretical range obtained by stellar population synthesis calculations (Bulik, Belczynski & Kalogera 2003). The predictions of the mass distribution, however, are sensitive to parameters that govern single and binary star evolution and still contain significant uncertainties. A comparison with observations of Galactic double NS binaries, which currently span a range of q-values between 0.67 and nearly unity [see the recent reviews by Lattimer & Prakash (2004) and Stairs (2004)] is therefore difficult and is also hampered by the still small number of detected NS+NS systems.

In the following analysis and discussion of our models, we have synchronized the time-axis to the time of maximal GW luminosity. This allows for a better comparison of the temporal evolution.

3 RESULTS OF MERGER MODELS

3.1 Dynamics of merging

The evolution of a NS binary during the adiabatic inspiral is driven by gravitational radiation reaction. Once the binary becomes unstable to tidal forces, the hydrodynamic evolution sets in, leading to the tidal stretching of one or of both companions and to the formation of a central hypermassive NS surrounded by a thick, neutron-rich accretion torus. Depending on its mass and rotation rate and the EoS, the hypermassive NS will collapse immediately or after a (short?) delay to a rapidly rotating BH (e.g. Morrison et al. 2004).

The dynamics and post-merging structure largely depend on the mass ratio q of the binary. In asymmetric systems with q significantly smaller than 1, the less massive but slightly larger star is tidally disrupted and deformed into an elongated primary spiral arm, which is mostly accreted on to the more massive companion. Its tail, however, contributes a major fraction to the subsequently forming thick disc/torus around a highly deformed and oscillating central remnant (see Fig. 1, Panels a and b). In systems with $q \simeq 1$ and nearly equally sized stars, both stars are tidally stretched but not disrupted and directly plunge together into a deformed merger remnant (see Fig. 2). In all models, excited radial and non-radial oscillations of the compact remnant periodically lead to mass shedding off the surface and to ejection of material into secondary tidal tails during the subsequent evolution. As illustrated in Figs 1 and 2, this effect takes place in both symmetric and asymmetric cases, but is stronger in the latter because of the larger triaxial deformation of the post-merger object.

Table 1. Parameters of the considered NS+NS models. M_1 and M_2 denote the individual gravitational masses of the NSs in isolation, while $M_{\rm sum} = M_1 + M_2$ stands for the sum of the two. Note that the total gravitational mass M is slightly smaller than $M_{\rm sum}$ because M also involves the negative gravitational binding energy between the two stars. M_0 is the total baryonic mass, $q = M_1/M_2$ and $q_{\rm M} = M_{0,1}/M_{0,2}$ are the gravitational and baryonic mass ratios, respectively. 'Shen' stands for the full, non-zero temperature EoS of Shen et al. (1998a,b), while 'Shen_c' denotes the $T = 0$ slice of this EoS table. Characteristic data of the post-merger system are read off at $t \sim 6$ ms. $M_{0,\rm disc}$ and $J_{\rm disc}$ are the baryonic mass and the angular momentum of the disc, respectively. $M_{\rm rem}$ is the remnant gravitational mass, and $a_{\rm rem} = (J_{\rm total} - J_{\rm disc})/M_{\rm rem}^2$ is the corresponding spin parameter. $j_{\rm ISCO}$ and $r_{\rm ISCO}$ are the specific angular momentum and the radius of the ISCO of a Kerr-BH with the gravitational mass and spin parameter of the remnant.

Model	$M_1(\rm M_\odot)$	$M_2(\rm M_\odot)$	$M_{\rm sum}(\rm M_\odot)$	$M_0(\rm M_\odot)$	q	$q_{\rm M}$	EoS	$M_{0,\rm disc}(\rm M_\odot)$	$J_{\rm disc}$ (10^{48} g cm^2 s^{-1})	$M_{\rm rem}(\rm M_\odot)$	$a_{\rm rem}$	$j_{\rm ISCO}$ (10^{16} cm^2 s^{-1})	$r_{\rm ISCO}$(km)
S1414	1.4	1.4	2.8	3.032	1.0	1.0	Shen	0.06	3.6	2.64	0.91	2.20	4.6
S138142	1.38	1.42	2.8	3.032	0.97	0.97	Shen	0.06	3.6	2.64	0.89	2.30	5.0
S135145	1.35	1.45	2.8	3.034	0.93	0.93	Shen	0.09	5.9	2.62	0.88	2.35	5.3
S1315	1.3	1.5	2.8	3.037	0.87	0.86	Shen	0.15	10	2.57	0.85	2.4	5.7
S1216	1.2	1.6	2.8	3.039	0.75	0.73	Shen	0.23	17	2.50	0.77	2.6	6.9
S1515	1.5	1.5	3.0	3.274	1.0	1.0	Shen	0.05	3.4	2.82	0.90	2.4	5.3
S1416	1.4	1.6	3.0	3.274	0.88	0.86	Shen	0.17	12	2.73	0.86	2.5	6.2
S1317	1.3	1.7	3.0	3.279	0.76	0.75	Shen	0.23	17	2.69	0.79	2.7	7.0
S119181	1.19	1.81	3.0	3.289	0.66	0.63	Shen	0.24	20	2.67	0.73	2.85	7.9
S107193	1.07	1.93	3.0	3.306	0.55	0.52	Shen	0.26	24	2.67	0.64	3.1	9.5
S1313	1.3	1.3	2.6	2.800	1.0	1.0	Shen	0.08	4.7	2.44	0.91	2.0	4.3
S1214	1.2	1.4	2.6	2.799	0.86	0.85	Shen	0.20	13	2.33	0.84	2.2	5.3
S1115	1.1	1.5	2.6	2.807	0.73	0.71	Shen	0.23	17	2.31	0.77	2.35	6.2
C1216	1.2	1.6	2.8	3.039	0.75	0.73	Shen_c	0.21	21	2.39	0.75	2.5	6.7
C1315	1.3	1.5	2.8	3.037	0.87	0.86	Shen_c	0.14	15	2.47	0.84	2.35	5.8

3.2 Disc formation

If and when the compact post-merger object collapses to a BH (the secular evolution driven by GW radiation reaction, viscosity and MHD cannot be followed by 3D simulations), pressure support from the central remnant to the disc will vanish, and matter will be prevented from infall mostly by rotational support. As a consequence, we distinguish future disc matter from the central remnant by demanding the specific angular momentum j to be larger than the one associated with the innermost stable circular orbit (ISCO) of a Kerr BH with the gravitational mass and the spin parameter of the central remnant.

The ISCO can be analytically determined in the case of the Boyer–Lindquist Kerr metric (Bardeen, Press & Teukolsky 1972). In our case, we will use an approximative pseudo-Kerr metric (see e.g. Grandclément, Gourgoulhon & Bonazzola 2002) which is both isotropic and conformally flat, consistent with the coordinates we used for our numerical simulations. The ISCO can then be found among all circular orbits in the orbital plane by minimizing the specific angular momentum along the radial coordinate.

Using this criterion, we are now able to identify the disc matter and disc mass for the various models considered. Their very different merger dynamics are reflected in the different evolution of the disc mass (see Fig. 3). The rapid rise in the asymmetric models around $t \simeq 0$ ms can be associated with the development of the primary spiral arm. After this dynamical phase shortly after merging, a nearly stationary torus forms, and the disc mass settles down to a slowly changing value, which is plotted versus mass ratio q for all models in Fig. 4. We find a rapid rise of the disc mass when q drops below unity, and a flattening for q-values below $\sim$0.8. The disc mass increases from about 0.05 $\rm M_\odot$ at $q = 1$ to about 0.26 $\rm M_\odot$ at $q = 0.55$.

We checked the consistency of our disc mass determination by comparing the obtained masses with the amount of matter residing outside the equatorial radius of the remnant $r_{\rm rem}$. We determine $r_{\rm rem}$ in a radial density profile by locating the point between the steep density gradient at the remnant surface and the slower fall-off in the disc. In all cases, we found $M_{\rm gas}(r > r_{\rm rem}) > M_{\rm gas}(j > j_{\rm ISCO}) \equiv M_{0,\rm disc}$, suggesting that gas pressure still plays an important role in the quasi-stationary phase. Our disc masses are therefore lower limits, since pressure support will not completely vanish even after the BH formation.

In Fig. 1, we have colour-coded for a $T = 0$ and a $T \neq 0$ model in red the material that belongs to the future disc, whereas the material that currently fulfils the disc criterion is shown in yellow. By definition, these two attributes coincide at the end of the simulation. We see that the future disc matter originates mainly from the spiral arm tips and the stellar surface. This indicates that the formation of a post-merger disc is linked to the presence of spiral arms. Indeed, the yellow tips of these tidal tails in Fig. 1, and also the enhanced specific angular momentum in the outer edges of the tidal tails in Fig. 5, suggest angular momentum transfer from the central remnant to the spiral arm tips via tidal torques. This hypothesis is confirmed by a post-processing analysis of Model C1216 where we integrated the torque exerted by gravitational and pressure forces from the compact deformed remnant on the yellow mass elements in the primary spiral arm as a function of time. The result for the total angular momentum evolution agrees very well with the simulation result (Fig. 6).

An interesting effect can also be seen by comparing models with $T = 0$ and $T \neq 0$ EoSs (Figs 1, 5 and 7) . In Fig. 7, we show the disc mass evolution of the cold Models C1216 and C1315 together with their non-zero temperature counterparts S1216 and S1315. Obviously, the first increase in disc mass, which can be associated with the cold primary spiral arm, is unaffected by temperature effects. Thermal pressure effects during the following evolution, however, reduce the further increase in disc mass in the non-zero temperature case, whereas in the cold case the disc mass increases by an additional $\sim 0.07\,\rm M_\odot$. We determine two possible reasons for this difference. On the one hand, the core of the cold merger remnant contracts more strongly due to the absence of thermal pressure.

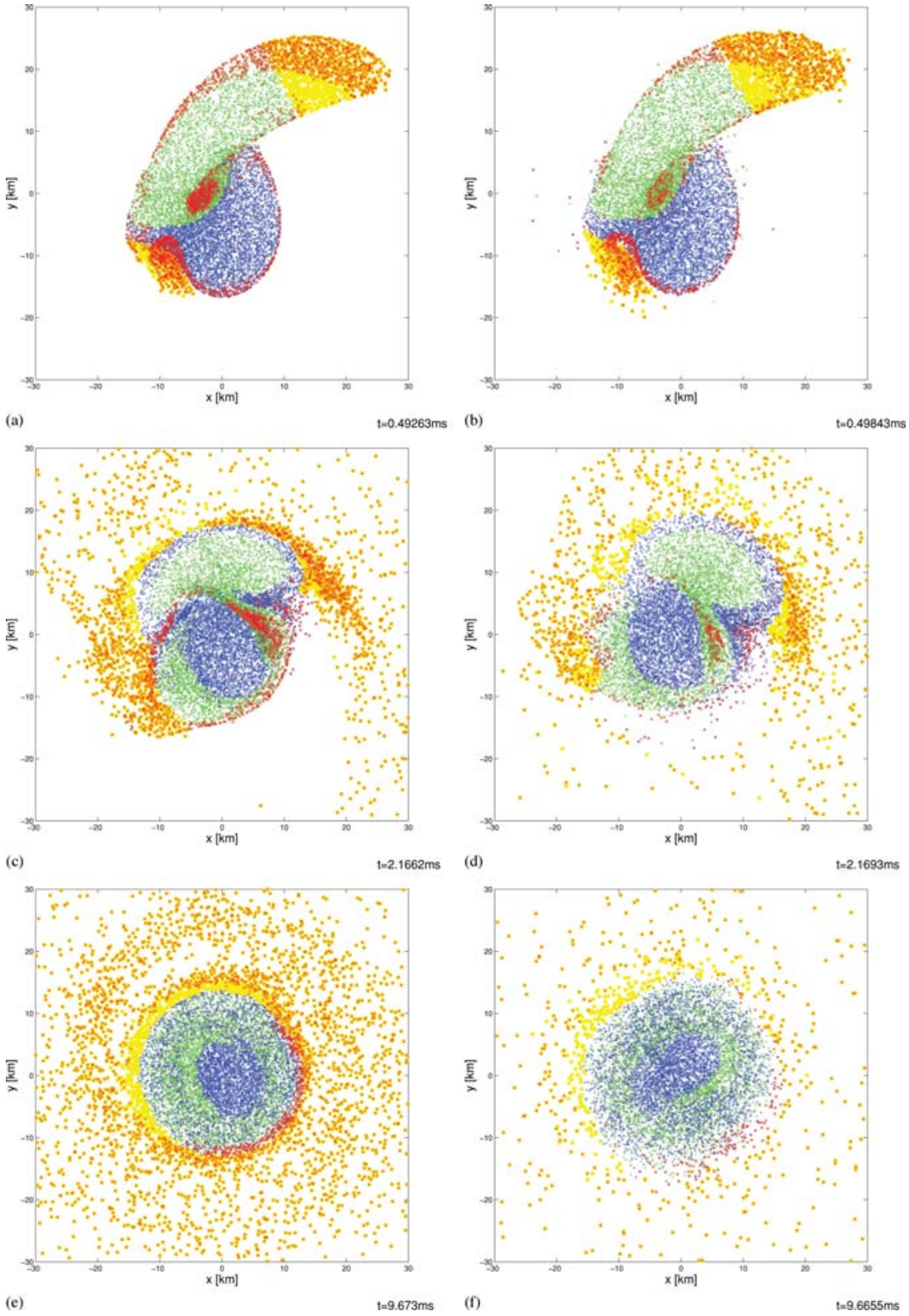

Figure 1. Characteristic evolutionary phases of Model C1216 (left-hand panels) and Model S1216 (right-hand panels). Panels (a) and (b) show the merging phase with a primary spiral arm forming. Plotted is every 10th SPH particle around the equatorial plane. The matter of the two stars is represented by green and blue particles, respectively. Particles that end up in the disc at the end of the simulation are marked in red, and the ones that currently fulfil the disc criterion (see Section 3.2) are plotted in yellow. Panels (c) and (d) display the situation ~ 2 ms after merging, when a secondary spiral arm appears. Panels (e) and (f) show the time when a quasi-stationary torus has formed. Note that the particle density is not strictly proportional to the density of the fluid because the particles near the initial stellar boundaries are attributed a smaller particle mass. These particles preferentially end up in the torus so that the particle density there appears enlarged.

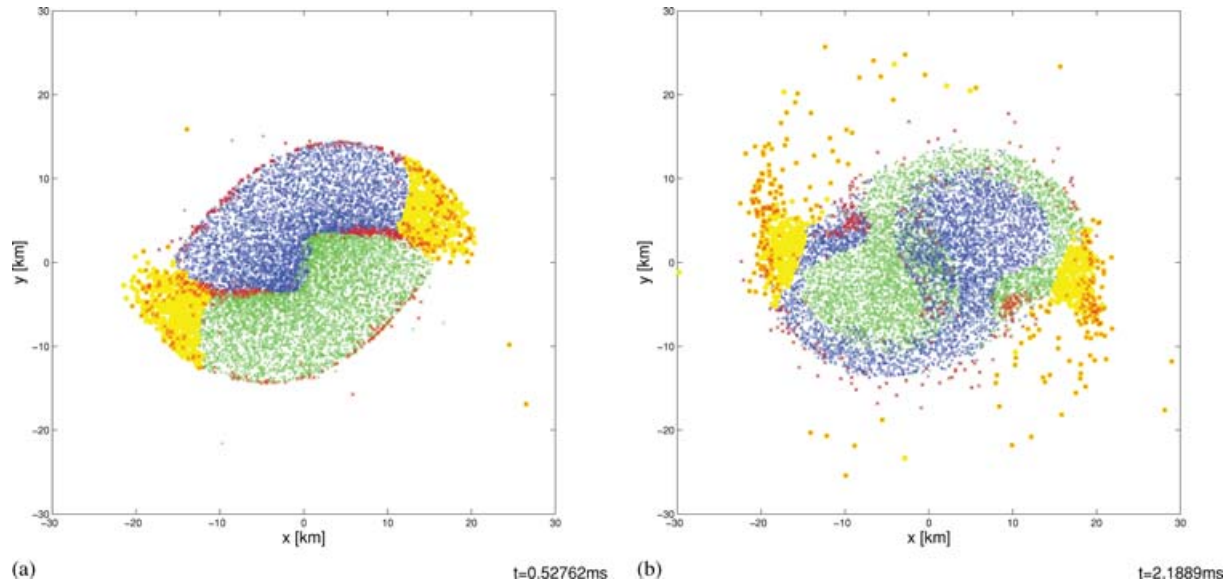

Figure 2. Same as Panels (a) and (c) and (b) and (d), respectively, of Fig. 1, but for Model S1414. The primary spiral arm is absent in the symmetric binary case and the post-merging (secondary) arms are smaller than in the asymmetric models.

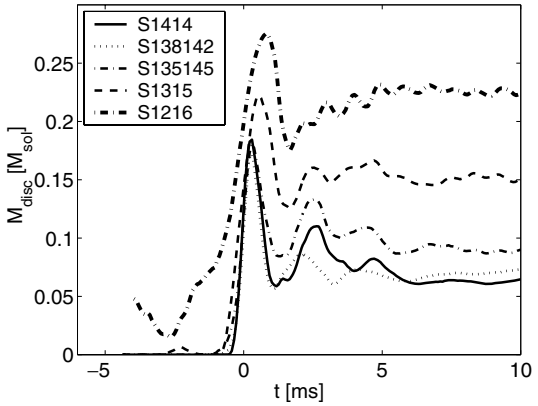

Figure 3. Disc formation in models with non-zero temperature EoS and $M_{\rm sum} = 2.8\,{\rm M}_{\odot}$. Plotted is the disc mass as inferred from our disc mass criterion (see text). The final disc mass as given in Table 1 is read off at about 6 ms. Clearly visible is the rapid rise at $t \simeq 0$, which depends strongly on the mass ratio. On the other hand, the further evolution after merging is similar in all cases.

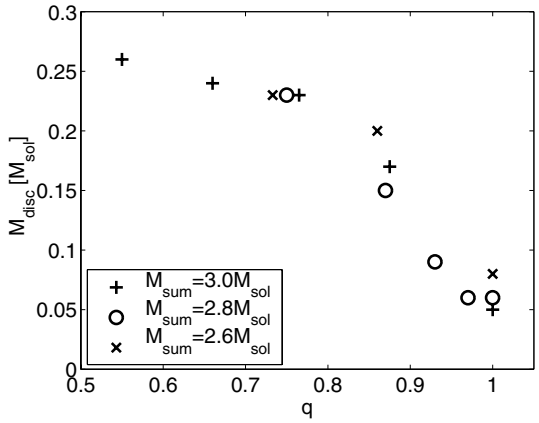

Figure 4. Disc masses versus mass ratio q for all non-zero temperature runs.

Therefore, more gravitational binding energy is converted into rotational energy and the rotation rates become higher, supporting the formation of spiral arms. On the other hand, the shock-heated matter from the collision region between the two NSs forms a halo of hot matter which engulfs the compact remnant–torus system in the $T \neq 0$ case (Figs 1 and 5). This halo may dampen the oscillations of the remnant and the development of large deviations from axisymmetry.

4 CONSTRAINTS FROM OBSERVED GRBS

In this section, we will discuss how the properties of the GRB engine may be constrained from the recent observations of four short-duration GRBs. To this end, we will make the assumption that the bursts originated from ultrarelativistic jets whose acceleration was mainly driven by thermal energy provided by the annihilation of neutrino-antineutrino ($\nu\bar{\nu}$) pairs in the vicinity of post-merger BH–torus systems (see e.g. Ruffert & Janka 1999; Setiawan, Ruffert & Janka 2004). Although we will refer to this scenario in our discussion because numerical models provide at least order of magnitude information of involved parameters, our arguments are more general and apply basically also to models that consider MHD-powered GRB jets.

4.1 BH–torus system parameters

Linking the measured apparent (i.e. isotropic-equivalent) energy $E_{\gamma,\rm iso}$ of a short GRB to the energy output from the central engine and the mass $M_{\rm acc}$ accreted by the BH (during the phase when the neutrino emission from the accretion torus is sufficiently powerful to drive the jets) involves a chain of efficiency parameters corresponding to the different steps of physical processes between the energy release near the BH and the gamma-ray emission at $\sim 10^{14}$ cm:

$$E_{\gamma,\rm iso} \;=\; f_1\, f_2\, f_3\, f_\Omega^{-1}\, f_4\, M_{\rm acc} c^2. \qquad (1)$$

Here, f_1 denotes the efficiency at which accreted rest mass energy can be converted to neutrino emission, f_2 is the conversion efficiency of neutrinos and antineutrinos by annihilation to $e^{\pm}$ pairs, f_3 is the

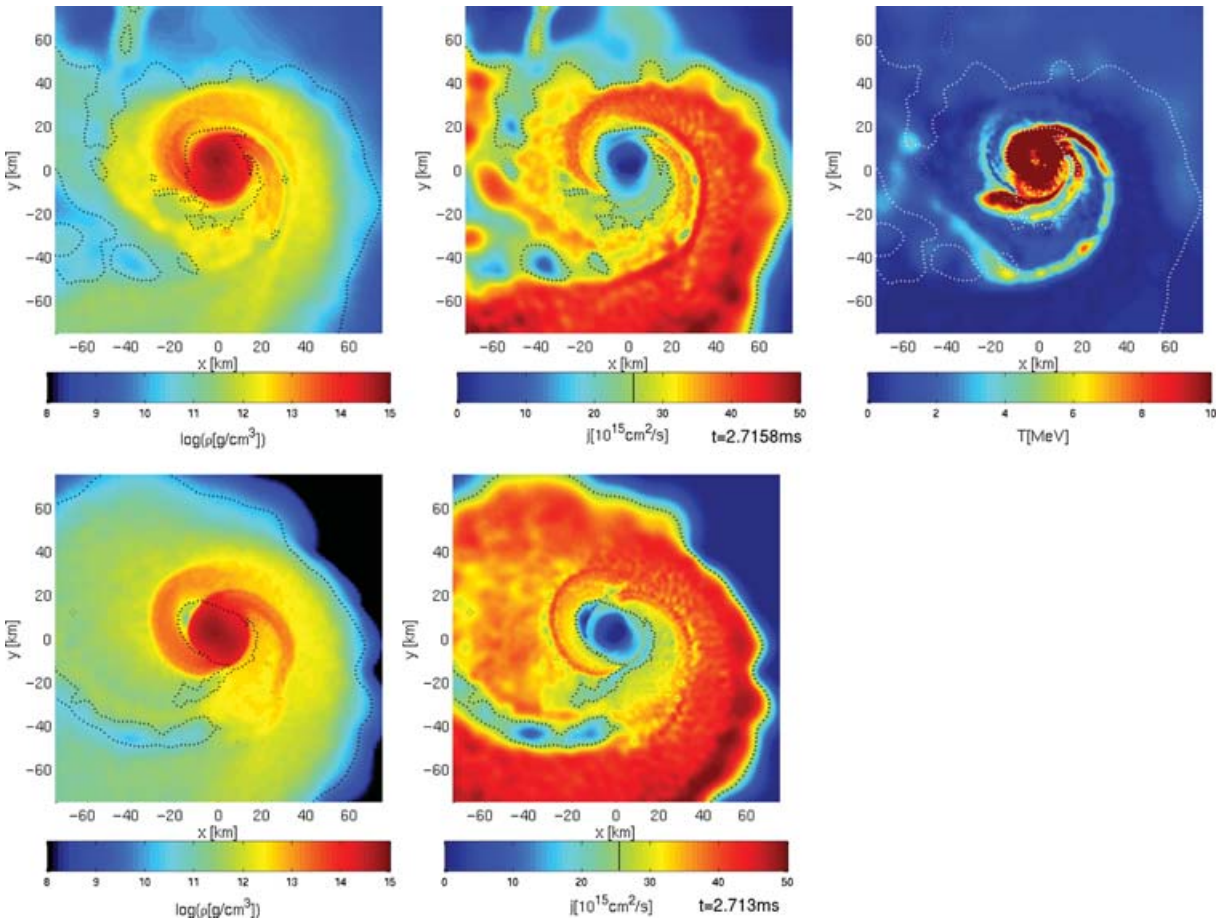

Figure 5. Density ρ (left), specific angular momentum j (middle) and temperature distribution T (right) in the orbital plane for the $T \neq 0$ Model S1216 (top) and the $T = 0$ Model C1216 (bottom, without temperature). The black dotted line in all panels and the black solid line in the colour bars for j correspond to the location where the specific angular momentum is equal to the value of $j_{\rm ISCO}$ at the given time (see text). Note that the colour bar for the upper right panel is limited to 10 MeV such that the temperature distribution in the disc becomes visible. The maximum temperature in the merger remnant rises up to ∼30 MeV at the given time.

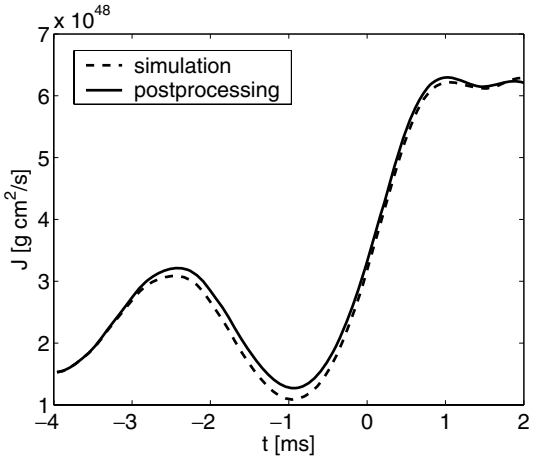

Figure 6. Total angular momentum of a blob of matter in the primary spiral arm of Model C1216. The dashed line represents the results of the simulation, and the solid line those of a post-processing analysis.

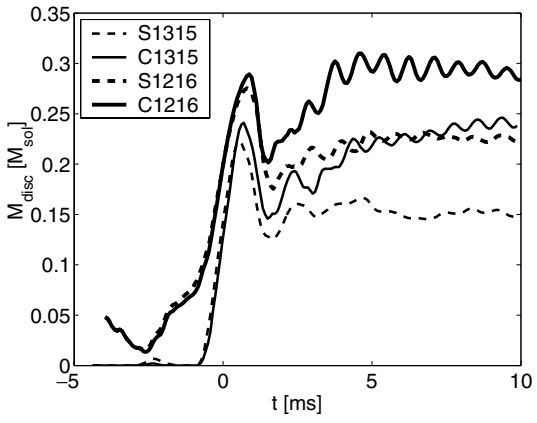

Figure 7. Same as in Fig. 3, but comparing the differences between $T = 0$ EoS and non-zero temperature EoS for two different mass ratios q.

fraction of the $e^{\pm}$-photon fireball energy which drives the ultrarelativistic outflow with the Lorentz factors $\Gamma > 100$ as required by GRBs, $f_\Omega = 2\Omega_{\rm jet}/(4\pi) = 1 - \cos\theta_{\rm jet}$ denotes the jet collimation factor defined as the fraction of the sky covered by the two polar jets (with semi-opening angles $\theta_{\rm jet}$ and solid angles $\Omega_{\rm jet}$) and f_4 is the fraction of the energy of ultrarelativistic jet matter which can be emitted in gamma rays in course of dissipative processes that occur in shocks when optically thin conditions are reached.

These parameters are constrained to some degree by numerical and analytic work, but their values are still rather uncertain and might

Table 2. Estimated accreted masses, $M_{\rm acc}$, and lower bounds for the average mass accretion rates, $\dot{M}_{\rm acc}$, assuming post-merger BH–torus systems being the energy sources of the recently observed, well-localized short GRBs. The estimates are based on equations (1) and (2). The quantity $E_{\gamma,\rm iso}$ is the isotropic-equivalent gamma-ray burst energy (corrected for the cosmological redshift z of the burst), and t_γ is the GRB duration at the source, computed as $t_\gamma = T_{90}/(1+z)$ from the measured 90 per cent inclusive interval of high-energy emission. The observational data were taken from Fox et al. (2005).

GRB	z	t_γ(s)	$E_{\gamma,\rm iso}$(erg)	$M_{\rm acc}(\rm M_\odot)$	$\dot{M}_{\rm acc}(\rm M_\odot/s)$
050509b	0.225	0.033	4.5×10^{48}	2.5×10^{-3}	0.08
050709	0.160	0.060	6.9×10^{49}	3.8×10^{-2}	0.6
050724	0.258	2.4	4.0×10^{50}	2.2×10^{-1}	0.09
050813	0.722	0.35	6.5×10^{50}	3.6×10^{-1}	1.0

vary strongly with time- and system-dependent conditions of the source. 'Typical' values from merger and accretion simulations are $f_1 \sim 0.05$ (Setiawan et al. 2004; Lee et al. 2005), $f_2 \sim 0.001, \ldots, 0.01$ (Ruffert & Janka 1999; Setiawan et al. 2004), $f_3 \sim 0.1$, $f_\Omega \sim 0.01, \ldots, 0.05$ and $f_4 \lesssim 0.2$ from estimates for internal shock models (Daigne & Mochkovitch 1998; Guetta, Spada & Waxman 2001; Kobayashi & Sari 2001, and references therein).

The cited values for f_3 and f_Ω were determined by relativistic hydrodynamical calculations of the formation and propagation of jets driven by thermal energy deposition around BH–torus systems (Aloy et al. 2005). These simulations revealed that about 10–30 per cent of the $e^\pm$-pair plasma fireball energy are used for hydrodynamically accelerating the baryonic matter in the jets to ultrarelativistic velocities. Typical jet half-opening angles were found to be between 10° and 15°, corresponding to $f_\Omega \sim 1.5 \times 10^{-2}, \ldots, 3.4 \times 10^{-2}$ (Aloy et al. 2005; Janka et al. 2005). Two of the four well-localized short GRBs indeed provide hints for this degree of collimation (see Berger et al. 2005; Fox et al. 2005) predicted by the theoretical work.

Because of the lack of detailed information about how the factors f_1 to f_4 and f_Ω depend on the properties of NS+NS binaries and their relic BH–torus systems, we made the simplifying and bold assumption that the set of parameter values is the same for all cases, $(f_1, f_2, f_3, f_\Omega, f_4) = (0.1, 0.01, 0.1, 0.01, 0.1)$, and applied equation (1) to the four observed short GRBs, using the measured isotropic-equivalent gamma-energies of Table 2. Doing so, we obtained the estimates listed in that table for the accreted mass $M_{\rm acc}$.[1] Assuming further that the duration t_γ of the GRB (at the location of the redshifted source) is an upper bound for the duration of the accretion of $M_{\rm acc}$ by the BH, $t_{\rm acc} \lesssim t_\gamma$ (cf. Aloy et al. 2005), we can deduce lower limits for the average mass accretion rates,

$$\dot{M}_{\rm acc} \gtrsim \frac{M_{\rm acc}}{t_\gamma}. \qquad (2)$$

These are also listed in Table 2 and plotted versus $M_{\rm acc}$ in Fig. 8. We obtain in all cases values for the torus masses in the range of

[1] Note that the (initial) torus mass may be larger than the accreted mass that we determine from the observed GRB properties. A part of the torus may fall into the BH without producing a release of energy which is strong enough to power ultrarelativistic GRB jets. Some part of the torus mass will also be ejected by winds driven by neutrino energy deposition (see e.g. Ruffert et al. 1997; Rosswog & Liebendörfer 2003), viscous heating or MHD effects (see e.g. Daigne & Mochkovitch 2002), and some part of the torus mass may be lost equatorially due to the outwards transport of angular momentum by viscous shear in the (magnetized) accretion torus.

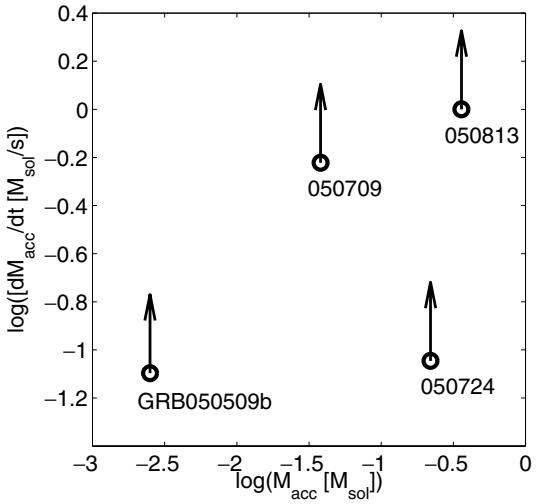

Figure 8. Estimated accreted masses, $M_{\rm acc}$, and lower bounds for the average mass accretion rates, $\dot{M}_{\rm acc}$ for the four well-localized short GRBs of Table 2.

those determined in this work (Fig. 4), and values for the mass accretion rates in the ballpark of theoretical expectations for post-merger BH accretion. Simulations of the latter find mass accretion rates of typically between several $0.1\,\rm M_\odot\,s^{-1}$ and several $\rm M_\odot\,s^{-1}$ (e.g. Ruffert & Janka 1999; Lee & Ramirez-Ruiz 2002; Setiawan et al. 2004; Lee et al. 2005). Of course, the numerical values for $M_{\rm acc}$ and $\dot{M}_{\rm acc}$ in Table 2 are very uncertain and have to be taken with caution. Shifts by factors of a few are easily possible because of probable system-dependent variations of the efficiency factors f_1 to f_4 and of the jet collimation factor f_Ω. Nevertheless, it is very encouraging that the simple and straightforward calculations based on equations (1) and (2) lead to reasonable numbers in all cases.

GRB 050509b, for example, is particularly interesting because of its very short intrinsic duration of $t_\gamma \sim 33$ ms and an extraordinarily low isotropic energy of a few 10^{48} erg if it is located at $z = 0.225$ (Gehrels et al. 2005). Such a low-energy event can be explained by the accretion of discs in the lower range of masses found here for symmetric NS+NS binaries, even when rather conservative assumptions are made for the incompletely known efficiencies of the various process steps between the energy release near the BH and the gamma-ray emission. We find that an accreted mass of 10^{-3}–10^{-2} $\rm M_\odot$ is well sufficient to account for the energetics of GRB 050509b. Of course, the mass could also be larger if the energy conversion to ultrarelativistic outflow and GRB emission is less efficient than we assumed.

4.2 Constraints from the low-energy, short-duration GRB 050509b

If further observations substantiate the link between NS+NS mergers and short GRBs, this may set constraints on the post-merging evolution and the nuclear EoS. On the one hand, the hypermassive NS should escape the collapse to a BH for a sufficiently long time so that an accretion torus can form by the described dynamical processes. On the other hand, the collapse of the hot, neutrino radiating NS should not be delayed too much because neutrino energy deposition in the surface-near layers of the NS will lead to a massive baryonic wind (Duncan et al. 1986; Woosley 1993a; Qian

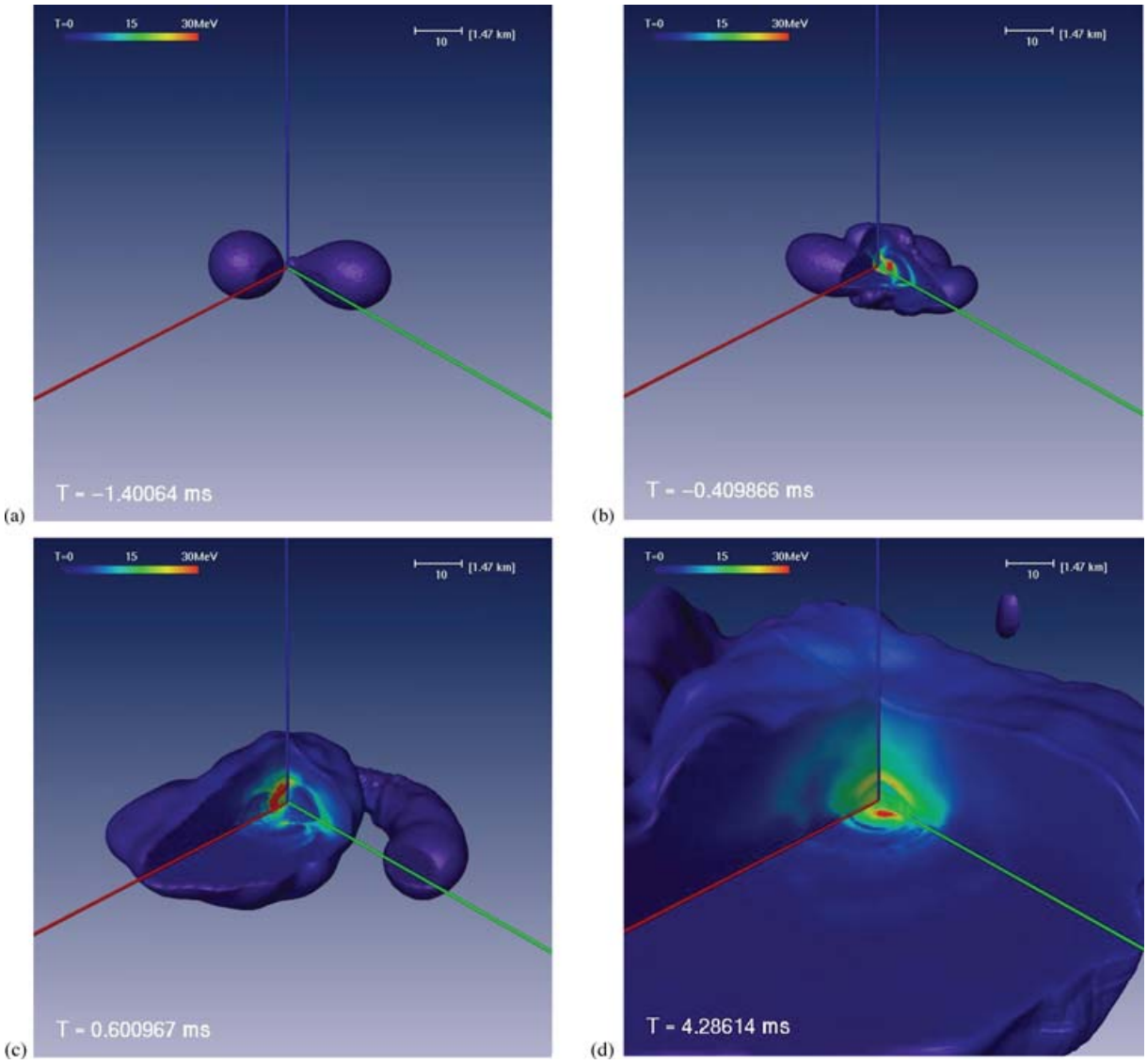

Figure 9. Four stages of the NS+NS merger Model S1216. The surface is chosen to correspond to a density of $10^{10}\,\mathrm{g\,cm^{-3}}$, the temperature distribution is visible colour coded in the octant cut out from the 3D mass distribution. Temperatures up to 30 MeV are reached at the centre only milliseconds after the two NSs have merged. Time is given in the lower left corner of the panels, and length is measured in units of 1.47 km (top right corner of each panel).

& Woosley 1996; Thompson, Burrows & Meyer 2001), which can seriously endanger the subsequent formation of a GRB jet or fireball.

The mass-loss rate of the neutrino radiating NS due to this non-relativistically expanding outflow of bayonic matter was estimated by Woosley (1993a) and Qian & Woosley (1996) and is approximately given by (see Heger, Woosley & Spruit 2005)

$$\dot{M}_{\mathrm{wind}} \approx 8.5\times10^{-3}\,L^{5/3}_{\nu_\mathrm{e}+\bar{\nu}_\mathrm{e},53}\,R^{5/3}_{30}\,M_3^{-2}\,\mathrm{M_\odot\,s^{-1}} \qquad (3)$$

where $L_{\nu_\mathrm{e}+\bar{\nu}_\mathrm{e},53}$ is the luminosity of electron neutrinos plus antineutrinos in units of $10^{53}\,\mathrm{erg\,s^{-1}}$, R_{30} the NS radius normalized to 30 km and M_3 the NS mass in units of $3\,\mathrm{M_\odot}$. This mass-loss rate can be up to $\sim10^{-2}\,\mathrm{M_\odot\,s^{-1}}$ for the neutrino luminosities found in NS+NS merger simulations and the masses and radii of the compact post-merger object (see Ruffert & Janka 2001; Rosswog & Ramirez-Ruiz 2002; Rosswog & Liebendörfer 2003). Upon colliding with each other, the two merging NSs heat up by shocks and compression to central temperatures of several 10 MeV (Figs 5 and 9). Within only a few milliseconds after the final plunge, the neutrino emission reaches luminosities of $10^{53}\,\mathrm{erg\,s^{-1}}$ or higher [for more information, see Ruffert et al. (1997); Ruffert & Janka (2001); Rosswog & Liebendörfer (2003); Rosswog & Ramirez-Ruiz (2003)], and the post-merger object should start losing mass in the neutrino-driven wind.[2] Equation (3), however, does not take into account the effects of the very rapid rotation of the NS on the wind. This question is still unexplored, but the rapid spinning of the remnant born in a NS+NS merger event may lead to changes of the functional dependence of $\dot{M}$ on the NS properties and may also imply a strong pole-to-equator difference of the mass-loss rate.

[2] The development of the neutrino-driven wind is not seen in current NS+NS merger simulations because it requires a suitable treatment of neutrino transport, whereas the present models describe neutrino effects with a trapping scheme at best, which releases neutrinos from the stellar medium according to their local production rates, properly reduced due to a finite diffusion time-scale (see Ruffert et al. 1996 and Rosswog & Liebendörfer 2003).

The non-relativistic wind will create an extended baryonic halo that surrounds the merger remnant, before the compact central part undergoes collapse to a BH and the outer, high-angular momentum matter assembles in a torus around the BH. A jet launched from such a system and expanding into the pre-existing wind halo may then sweep up so much mass – even if the halo has a low density and small mass – that the high Lorentz factor outflow needed for GRBs ($\Gamma \gtrsim 100$) is prevented. This was, for example, seen in the type-A models of Aloy et al. (2005). A rather fast collapse of the relic hot, supramassive or hypermassive remnant to a BH is therefore required, if the cloud of baryonic matter produced by the neutrino-driven wind from the transiently stable NS will not become such a hazard for the GRB.[3]

A corresponding mass limit for the wind halo around the newly formed BH–torus system can be derived by the following arguments. In order for the baryon loading to remain sufficiently low so that acceleration to the Lorentz factors above a value Γ_0 (100 or more) is possible, the mass of the halo swept up by two relativistic GRB jets, $M_{\rm swept}$, is constrained by the condition $E_{\rm kin}(\Gamma > \Gamma_0)/(M_{\rm swept}\, c^2) > \Gamma_0$. Here, $E_{\rm kin}(\Gamma > \Gamma_0)$ is the kinetic energy of matter which can accelerate to Lorentz factors larger than Γ_0 in the two polar jets that expand away from the BH in the axial direction. For a jet collimation factor f_Ω, this kinetic energy is linked to the isotropic equivalent γ-energy of the GRB by $E_{\rm kin} = E_{\gamma,{\rm iso}}\, f_\Omega / f_4$, when f_4 is again the efficiency for the conversion of kinetic energy to gamma rays. On the other hand, the wind mass swept-up by the jets is given as $M_{\rm swept} = f_\Omega \alpha M_{\rm wind}$, where $M_{\rm wind} \approx \dot{M}_{\rm wind} t_{\rm NS}$ is the mass of the wind for a lifetime $t_{\rm NS}$ of the NS, and $\alpha < 1$ is a fudge factor which accounts for the fact that the wind from a rapidly rotating NS might be less dense along the rotation axis than calculated from equation (3). Combining all, we get the condition

$$t_{\rm NS} \lesssim \frac{E_{\gamma,{\rm iso}}}{\Gamma_0\, f_4\, \alpha\, \dot{M}_{\rm wind}\, c^2}\,. \qquad (4)$$

With $\Gamma_0 = 100$, $f_4 \sim 0.1$, $\dot{M}_{\rm wind} = 10^{-3}\,{\rm M}_\odot\,{\rm s}^{-1}$ (this assumption is on the low side of reasonable numbers from equation 3), and $E_{\gamma,{\rm iso}}$ from Table 2, we find for GRB 050509b (the lowest-energy case and thus the one providing the strongest limits) that $t_{\rm NS} < 1$ ms, assuming $\alpha = 1$. This means that due to the low energy of GRB 050509b even a tiny amount of baryonic pollution by swept-up wind matter would have prevented ultrarelativistic motion of the jets. The neutrino radiating merger remnant therefore must have collapsed to a BH essentially immediately after the binary NS merging and the onset of the neutrino-driven wind. Since it cannot be excluded that the density of the neutrino-driven wind along the rotation axis is much lower than estimated by equation (3), a more conservative estimate with $\alpha \sim 0.01$ yields $t_{\rm NS} < 100$ ms.

If GRB 050509b originated from a NS+NS merger, this result therefore suggests that the merger remnant was a hypermassive object, which was transiently stabilized by its rapid and differential rotation (Baumgarte, Shapiro & Shibata 2000), but had a very short lifetime. Referring to the analysis by Morrison et al. (2004) (see their table 2), this can either mean (i) that, if the high-density EoS was stiff, the system mass of the merging binary was unusually high compared to the known galactic double neutron stars, which all possess combined masses in the range of $M_{\rm sum} = M_1 + M_2 = 2.6$–$2.8\,{\rm M}_\odot$ (Stairs 2004); or, alternatively, (ii) that the nuclear equation of state is so soft that it could not support the merger remnant despite of its rapid differential rotation and thermal pressure; or (iii) that a very efficient mechanism was at work which destroyed the differential rotation of the compact remnant and extracted a sizable amount of its angular momentum on the required short time-scale. This could, for example, happen by hydrodynamical effects and mass shedding and/or by strong GW emission (Shibata et al. 2005).

Case (i) might be rejected as unlikely. Case (ii) tends to favour the 'softest' of the EoSs surveyed by Morrison et al. (2004) which support non-rotating NSs only up to a gravitational mass around $1.65\,{\rm M}_\odot$. Such EoSs, however, are excluded by the recent accurate measurement of a mass of $2.1\,{\rm M}_\odot$ for the millisecond pulsar PSR J0751+1807 (Nice et al. 2005) and by other neutron stars with masses beyond $2\,{\rm M}_\odot$ [see e.g. the review by Lattimer & Prakash (2004)]. An EoS which is sufficiently stiff to fulfil this observational constraint can also ensure the transient stability of the merger remnant of binary NS systems with a canonical mass of 2.6–$2.8\,{\rm M}_\odot$ [see the discussion of the critical mass for hypermassive NSs by Shibata et al. (2005)]. Therefore Case (iii) seems to offer a plausible scenario for GRB 050509b. The NS+NS binary had a typical mass, and the merger remnant was well above the maximum mass of stable, rigidly rotating NSs. The redistribution of angular momentum by non-axisymmetric hydrodynamic interaction and gravitational radiation (Shibata et al. 2005) or by viscosity and MHD effects (Shapiro 2000) has then driven the hypermassive object to gravitational instability on a time-scale of $\ll 100$ ms. The short accretion time-scale ($t_{\rm acc} < t_\gamma$) suggests that the remaining torus mass was small. This is consistent with our conclusion that little mass was accreted by the BH, which we have drawn from the low energy of GRB 050509b (Table 2). And it is consistent with the requirement coming from optical limits that little radiating material was ejected (Hjorth et al. 2005a), e.g. by neutrino-driven winds or by mass shedding due to viscous transport of angular momentum within the accretion torus. In view of the torus formation models presented here, this points to a symmetric or nearly symmetric NS+NS binary with a typical mass as the source of GRB 050509b.

5 DISCUSSION

Although our analysis of the four well-localized short GRBs was based on a number of unsettled assumptions, we found that the measured GRB energies and durations lead to estimates for $M_{\rm acc}$ and $\dot{M}_{\rm acc}$ that are roughly consistent with expectations from theoretical models of NS merging and post-merging evolution. However, in spite of this amazing result we think that it would be premature to claim that relic BH–torus systems from binary NS mergers and their associated neutrino emission can power all short GRBs.

Short GRBs have durations between a few milliseconds and about 2 s, and they might differ in their energy output by a factor of 100 or more. Observations also reveal large differences with respect to

[3] Note that neutrino energy deposition will later on also drive a baryonic wind off the accretion torus, after the latter was heated by viscous dissipation of rotational energy and has started to radiate neutrinos with high luminosities [see the discussion in Ruffert et al. (1997); Ruffert & Janka (1999); Rosswog & Ramirez-Ruiz (2002); Rosswog et al. (2003), and find information about the neutrino emission from such accretion tori in Setiawan et al. (2004) and Lee et al. (2005), and references therein]. This wind does not provide such a hazard for GRB-viable outflows, because it originates from outside the ISCO, and angular momentum conservation prevents it from filling the axial regions above the poles of the BH. In fact, Rosswog et al. (2003) and Rosswog & Ramirez-Ruiz (2003) consider the pressure of such a 'wind envelope' as helpful for the collimation of a $\nu\bar{\nu}$-annihilation-driven axial jet (see Levinson & Eichler 2000), an effect which turned out to be secondary for getting collimated, highly relativistic outflow from BH–torus systems in recent hydrodynamical jet simulations (Aloy et al. 2005).

their light curves and spectral hardness ratios. This wide range of short GRB properties leaves plenty of room for the possibility that different compact binaries contribute to the observed events. For example, not only NS+NS but also NS+BH mergers can lead to BH–torus systems with sizable torus masses and favourable properties for GRB production. Even the physical processes which play a dominant role in the energy release of the central engine and jet formation might differ between the events. In fact, it might turn out that this is needed to account for the observed diversity of short GRBs and their afterglows. Flare-like events followed by a very rapid decay were, for example, observed in case of GRB 050724 hundreds of seconds after the initial GRB. This was interpreted as a consequence of long-time activity of the central engine, which might point to a partial disruption and gradual accretion of a NS by a BH (Barthelmy et al. 2005). Episodic and long-lasting mass transfer from the NS to the BH was found to be possible for certain NS/BH mass ratios in combination with special properties of the NS EoS (see e.g. Kluzniak & Lee 1998; Portegies Zwart 1998; Janka et al. 1999; Lee & Kluzniak 1999; Rosswog, Speith & Wynn 2004; Rosswog 2005; Davies, Levan & King 2005).[4]

The rather uncertain estimates of the merger rates also allow for the possibility that not all NS+NS/BH mergers produce GRBs [see e.g. Guetta & Piran (2005), taking into account that the hydrodynamic models by Aloy et al. (2005) yield jet semi-opening angles of $\sim 10^\circ$ instead of a value of $\sim 1^\circ$ as found by Guetta & Piran with the assumption that all mergers make GRBs].

We therefore refrain (unlike other; see e.g. Lee et al. 2005; Rosswog & Ramirez-Ruiz 2003) from making predictions of the distribution of GRB properties on grounds of current simulations of NS+NS or NS+BH mergers. Such attempts are seriously hampered by the large number of unknowns in the theoretical picture and in particular their relation to the properties of compact object mergers.

(i) The distributions of binary parameters (NS and BH masses and spins, binary mass ratios) are highly uncertain. Theoretically, because of our incomplete understanding of the binary formation and evolution and of the supernova explosions which terminate the lives of massive stars and give birth to NSs (Bulik et al. 2003). And observationally, because of the rather limited sample of known NS+NS or NS+BH binaries (e.g. Lattimer & Prakash 2004; Stairs 2004). The latter aspect is particularly bothersome in view of the fact that only a minor fraction (of the order of 10 per cent?) of NS+NS/BH mergers might be able to produce GRBs and might be needed to account for the observed short bursts.

(ii) NS+NS/BH merger models require much more work. Relativistic simulations of compact object mergers are needed for different (non-zero temperature) nuclear equations of state and different parameters of the binary systems. A softer nuclear EoS, for example, might lead to a relation between binary parameters and torus masses that differs from the results of this work, which are based on the rather stiff EoS of Shen et al. (1998a,b). NS+NS merger models must be consistently evolved from the last stages of the progenitor system, through the moment of BH formation, to the subsequent accretion and jet production phase, including all the potentially relevant physics like neutrino transport and magnetic fields. Only then, for example, will the question be answered under which circumstances the neutrino-driven wind from the transiently stable hypermassive merger remnant represents an unsurmountable obstacle for GRB jets.

(iii) The complex sequence of physical processes from the energy release by the merger remnant to the stage of GRB production involves large uncertainties, expressed by the product of efficiency factors f_1 to f_4 and jet collimation factor f_Ω, which appears in equation (1). Each of these factors can contain still unknown dependences on the parameters of the NS+NS/BH binary and of its relic BH–torus system. Improved simulations of jet formation by energy release around post-merger BH–torus systems are necessary to clarify these dependences.

(iv) Since the compact proto-BHs found in our NS+NS merger simulations have significant angular momentum ($a_{\rm rem}$ is between 0.64 and 0.91 for the considered mergers of irrotational binaries; Table 1), the energy release during the accretion is likely to be boosted by Kerr effects. Not only may neutrino emission and neutrino-antineutrino annihilation play a role, but energy release through magnetic processes may also play a role, e.g. by the Blandford–Znajek (1977) mechanism (see e.g. Lee et al. 2005).

Much more theoretical work and numerical modelling are therefore needed before truly meaningful and reliable theoretical predictions of GRB properties and their link to NS+NS/BH merger parameters will become possible. Such predictions need to invoke, in particular, detailed models of the structure of the collimated ultrarelativistic outflows from the merger remnants and assumptions about the production of the GRB emission at large distances. Detailed consideration of the relevant physics is clearly beyond the scope of this paper. A first, still very crude attempt to employ such calculations of jets from BH–torus systems for predicting the distributions of observable GRB properties has been attempted recently by Janka et al. (2005).

6 SUMMARY AND CONCLUSIONS

We have shown that non-radial oscillations and triaxial deformation and the associated tidal torques can mediate efficient angular momentum transfer in the compact remnant within the first milliseconds after the merging of two NSs. Applying different criteria, we estimated the mass of the torus which will survive the future collapse of the central, dense object to a BH. For the considered irrotational systems and the employed relatively stiff nuclear EoS of Shen et al. (1998a,b), we determined lower disc mass limits of 1–2 per cent of the (baryonic) system mass for a NS–NS (gravitational) mass ratio around $q = 1$, increasing to about 9 per cent for systems with q around 0.55. Though the disc mass is more sensitive to the parameter q, we also observed a mild inverse relation between torus mass and binary system mass. For the same value of q, slightly higher torus masses were found when $M_{\rm sum} = M_1 + M_2$ was lower (Fig. 4). Non-zero temperature effects turned out to be important and to *reduce* the disc mass by several 10 per cent compared to the values for the $T = 0$ case.

The disc masses obtained in our simulations confirm the viability of post-merging BH–torus systems as central engines of short GRBs, and they support the theoretical possibility that thermal energy deposition above the poles of the BH by $\nu\bar{\nu}$ annihilation could be the primary energy source of short GRBs. The ultrarelativistic outflow of matter powered by this energy deposition was found in hydrodynamic simulations to be highly collimated in jets with semi-opening angles between about 10° and 15° (Aloy et al. 2005). This

[4] Simulations and analytic studies of NS+BH mergers have so far been carried out only in Newtonian gravity and disregarding the probable rotation of the BH. A Newtonian treatment, however, does not reproduce the correct mass–radius relation of a relativistic NS, for example. Current predictions of the merger evolution and of the dynamics of disc formation and accretion in such extremely relativistic systems therefore cannot be considered as reliable and conclusive, neither quantitatively nor qualitatively.

prediction seems to be supported by the observations of two of the four recently detected well-localized, short, hard GRBs (Fox et al. 2005).

Using typical parameters that describe the multi-step process from the energy release of the central engine to the observed GRB in this scenario, we derived estimates of the accreted masses and mass accretion rates (see Table 2) from the measured GRB energies and durations, using equations (1) and (2). For all cases, we found values for $M_{\rm acc}$ and $\dot{M}_{\rm acc}$ that are in the ballpark of the expectations from our NS+NS merger models and from models of BH accretion in post-merging BH–torus systems. Employing the same assumptions about the GRB engine, the extraordinarily low-energetic and short-duration GRB 050509b can be used to set strict limits for the lifetime of the post-merger hypermassive NS. It must have collapsed to a BH in much less than 100 ms with only little matter ($\sim$0.01 $M_\odot$) remaining in a torus around the BH to partially produce GRB-viable outflow. This favours a symmetric or nearly symmetric NS+NS binary as progenitor system, with a mass typical of the known galactic double NSs.

The knowledge of the binary system parameters, which could be obtained from the measurements of the GW chirp signal during the inspiral might allow one to deduce interesting information about the properties of the NS EoS from future short GRBs with determined distances. Constraining the EoS of NS matter by lifetime arguments for the supramassive or hypermassive remnant of NS+NS mergers, however, will require detailed relativistic models of the NS merging and of the post-merging evolution for different non-zero temperature EoSs, including the effects of magnetic fields (Shibata et al. 2005). GRB 050509b provides particularly strict limits in such an analysis, but may be a rare event where an exceptionally low-energy GRB with very short duration could be well localized.

ACKNOWLEDGMENTS

We thank M.A. Aloy for inspiring discussions and A. Marek for preparing the EoS table used in this work. Support from the Sonderforschungsbereich-Transregio 7 of the Deutsche Forschungsgemeinschaft is acknowledged. The computations were performed at the Rechenzentrum Garching.

REFERENCES

Aloy M. A., Janka H.-T., Müller E., 2005, A&A, 436, 273
Bardeen J. M., Press W. H., Teukolsky S. A., 1972, ApJ, 178, 347
Barthelmy S., 2005, Nat, 438, 994
Baumgarte T. W., Shapiro S. L., 2003, Phys. Rep., 376, 41
Baumgarte T. W., Shapiro S. L., Shibata M., 2000, ApJ, 528, L29
Berger E. et al., 2005, Nat, 438, 988
Blandford R., Znajek R., 1977, MNRAS, 179, 433
Blinnikov S., Novikov I., Perevodchikova T., Polnarev A., 1984, Sov. Astron. Lett., 10, 177
Bloom J. S. et al., 2006, ApJ, 638, 354
Brown G., Lee C.-H., Wijers R., Lee H., Israelian G., Bethe H., 2000, New Astron., 5, 191
Bulik T., Belczynski K., Kalogera V., 2003, in Cruise M., Saulson P., eds, Gravitational Wave Detection. Proceedings of the SPIE Vol. 4856, p. 146
Daigne F., Mochkovitch R., 1998, MNRAS, 296, 275
Daigne F., Mochkovitch R., 2002, A&A, 388, 189
Davies M., Levan A., King A., 2005, MNRAS, 356, 54
Drenkhahn G., Spruit H., 2002, A&A, 391, 1141
Duez M., Liu T., Shapiro S., Stephens B., 2004, Phys. Rev. D, 69, 104030
Duez M., Liu T., Shapiro S., Shibata M., Stephens B., 2005, Phys. Rev. Lett., 96, 031101
Duncan R. C., Shapiro S. L., Wasserman I., 1986, ApJ, 309, 141
Eichler D., Livio M., Piran T., Schramm D., 1989, Nat, 340, 126
Fox D. et al., 2005, Nat, 437, 845
Gehrels N. et al., 2005, Nat, 437, 851
Grandclément P., Gourgoulhon E., Bonazzola S., 2002, Phys. Rev. D, 65, 044021
Guetta D., Piran T., 2005, A&A, 435, 421
Guetta D., Spada M., Waxman E., 2001, ApJ, 557, 399
Heger A., Woosley S., Spruit H., 2005, ApJ, 626, 350
Hjorth J. et al., 2005a, ApJ, 630, L117
Hjorth J. et al., 2005b, Nat, 437, 859
Isenberg J., Nester J., 1980, in Held A., ed., General Relativity and Gravitation Vol. 1, Waveless Approximation Theories of Gravity. Plenum Press, New York, p. 23
Janka H.-T., Eberl T., Ruffert M., Fryer C., 1999, ApJ, 527, L39
Janka H.-T., Mazzali P., Aloy M.-A., Pian E., 2005, ApJ, submitted (astro-ph/0509722)
Jaroszyński M., 1993, Acta Astron., 43, 183
Kluzniak W., Lee W.-H., 1998, ApJ, 494, L53
Kobayashi S., Sari R., 2001, ApJ, 551, 934
Lattimer J., Prakash M., 2004, Science, 304, 536
Lee W.-H., Kluzniak W., 1999, ApJ, 526, 178
Lee W.-H., Ramirez-Ruiz E., 2002, ApJ, 577, 893
Lee W.-H., Ramirez-Ruiz E., Granot J., 2005, ApJ, 630, L165
Lee W.-H., Ramirez-Ruiz E., Page D., 2005, ApJ, 632, 421
Levinson A., Eichler D., 2000, Phys. Rev. Lett., 85, 236
Mochkovitch R., Hernanz M., Isern J., Martin X., 1993, Nat, 361, 236
Morrison I., Baumgarte T., Shapiro S., 2004, ApJ, 610, 941
Narayan R., Paczyński B., Piran T., 1992, ApJ, 395, L83
Nice D., Splaver E., Stairs I., Loehmer O., Jessner A., Kramer M., Cordes J., 2005, ApJ, 634, 1242
Oechslin R., Rosswog S., Thielemann F.-K., 2002, Phys. Rev. D, 65, 103005
Oechslin R., Uryū K., Poghosyan G., Thielemann F.-K., 2004, MNRAS, 349, 1469
Paczyński B., 1986, ApJ, 308, L43
Paczyński B., 1991, Acta Astron., 41, 257
Popham R., Woosley S., Fryer C., 1999, ApJ, 518, 356
Portegies Zwart S., 1998, ApJ, 503, L53
Qian Y.-Z., Woosley S., 1996, ApJ, 471, 331
Rosswog S., 2005, ApJ, 634, 1202
Rosswog S., Ramirez-Ruiz E., 2002, MNRAS, 336, L7
Rosswog S., Liebendörfer M., 2003, MNRAS, 342, 673
Rosswog S., Ramirez-Ruiz E., 2003, MNRAS, 343, L36
Rosswog S., Ramirez-Ruiz E., Davies M., 2003, MNRAS, 345, 1077
Rosswog S., Speith R., Wynn G., 2004, MNRAS, 351, 1121
Ruffert M., Janka H.-T., 1999, A&A, 344, 573
Ruffert M., Janka H.-T., 2001, A&A, 380, 544
Ruffert M., Janka H.-T., Schäfer G., 1996, A&A, 311, 532
Ruffert M., Janka H.-T., Takahashi K., Schäfer G., 1997, A&A, 319, 122
Setiawan S., Ruffert M., Janka H.-T., 2004, MNRAS, 352, 753
Shapiro S., 2000, ApJ, 544, 397
Shen H., Toki H., Oyamatsu K., Sumiyoshi K., 1998a, Nucl. Phys. A, 637, 435
Shen H., Toki H., Oyamatsu K., Sumiyoshi K., 1998b, Prog. Theor. Phys., 100, 1013
Shibata M., Taniguchi K., Uryū K., 2003, Phys. Rev. D, 68, 084020
Shibata M., Duez M., Liu T., Shapiro S., Stephens B., 2006, Phys. Rev. Lett., 96, 031102
Shibata M., Taniguchi K., Uryū K., 2005, Phys. Rev. D, 71, 084021
Stairs I., 2004, Science, 304, 547
Thompson T., Burrows A., Meyer B., 2001, ApJ, 562, 887
Villasenor J. et al., 2005, Nat, 437, 855
Wilson J., Matthews G., Marronetti P., 1996, Phys. Rev. D, 54, 1317
Woosley S., 1993a, ApJS, 97, 205
Woosley S., 1993b, ApJ, 405, 273
Woosley S., Baron E., 1992, ApJ, 391, 228

This paper has been typeset from a TEX/LATEX file prepared by the author.